

GAZEFORMER-MOE: CONTEXT-AWARE GAZE ESTIMATION VIA CLIP AND MOE TRANSFORMER

Xinyuan Zhao¹, Xianrui Chen¹, Ahmad Chaddad^{1,2,*}

¹AIPM, School of Artificial Intelligence, Guilin University of Electronic Technology, China

²Laboratory for Imagery, Vision and Artificial Intelligence, École de Technologie Supérieure, Canada

*Correspondence: ahmad8chaddad@gmail.com

ABSTRACT

We present a semantics modulated, multi scale Transformer for 3D gaze estimation. Our model conditions CLIP global features with learnable prototype banks (illumination, head pose, background, direction), fuses these prototype-enriched global vectors with CLIP patch tokens and high-resolution CNN tokens in a unified attention space, and replaces several FFN blocks with routed/shared Mixture of Experts to increase conditional capacity. Evaluated on MPIIFaceGaze, EYEDIAP, Gaze360 and ETH-XGaze, our model achieves new state of the art angular errors of 2.49° , 3.22° , 10.16° , and 1.44° , demonstrating up to a 64% relative improvement over previously reported results. ablations attribute gains to prototype conditioning, cross scale fusion, MoE and hyperparameter. Our code is publicly available at <https://github.com/AIPMLab/Gazeformer>.

Index Terms— Gaze estimation; multi scale fusion; MoE transformer

1. INTRODUCTION

Gaze estimation is an important task in the field of human-computer interaction (HCI), virtual and augmented reality (VR/AR), and learning analytics. It involves recovering a 3D line of sight or a 2D point of regard from images, enabling non-intrusive tracking of attention [1–4]. Recent advances in deep learning have taken advantage of full-face input to benefit from explicit head pose signals [5, 6], although this can introduce variability due to person-specific morphology, background clutter, and varying illumination, which harms robustness to appearance variation and cross-condition performance [7]. CLIP offers alignment of semantic priors that can be integrated without additional annotations [8]. Sparse Mixture-of-Experts (MoE) modules enhance conditional capacity efficiently by engaging a selective set of experts for each token [9, 10]. However, current frameworks frequently

lack the capability for targeted, sample-wise semantic modulation or fail to synthesize global semantics with mid- and fine-grained tokens, coupled with adaptive expert routing [5]. In response, we introduce GazeFormer-MoE, a streamlined framework that conditions CLIP global features via learned prototype banks, merges these enriched global vectors with CLIP patch and high-resolution CNN tokens within a unified Transformer model, and applies a routed/shared MoE for diversified appearance handling. This innovative design improves robustness against changes in illumination, pose, and background, while preserving interpretability. Our contributions are summarized as follows.

- 1. Method.** We propose a semantics-modulated multi scale pipeline that injects CLIP aligned, learnable prototypes into global features and jointly attends prototype-enriched global vectors, CLIP patch tokens and high-resolution CNN tokens within a single Transformer encoder.
- 2. Architecture.** We design a routed and shared MoE Transformer that combines specialized experts for rare appearance sub distributions with shared experts for stability, increasing modeling capacity without uniformly increasing dense parameters.
- 3. Evaluation.** We adhere to the benchmark defined in a recent review of gaze estimation [5], and based on this, attains new state of the art (SOTA) results on four existing benchmarks.

The remainder of this paper is organized as follows. Section 2 formalizes the gaze estimation task and details our approach, including CLIP prototype selection, unified multi scale token fusion, and routed/shared MoE Transformer design. Section 3 presents datasets, implementation details, and training protocols. Section 4 provides a comprehensive discussion, and Section 5 summarizes the study.

2. METHODOLOGY

We present GazeFormer-MoE, a multi-modal Transformer that combines CLIP-driven semantic context, patch-level to-

This research was funded by the National Natural Science Foundation of China grant number 82260360, and the Guangxi Science and Technology Base and Talent Project (2022AC18004, 2022AC21040).

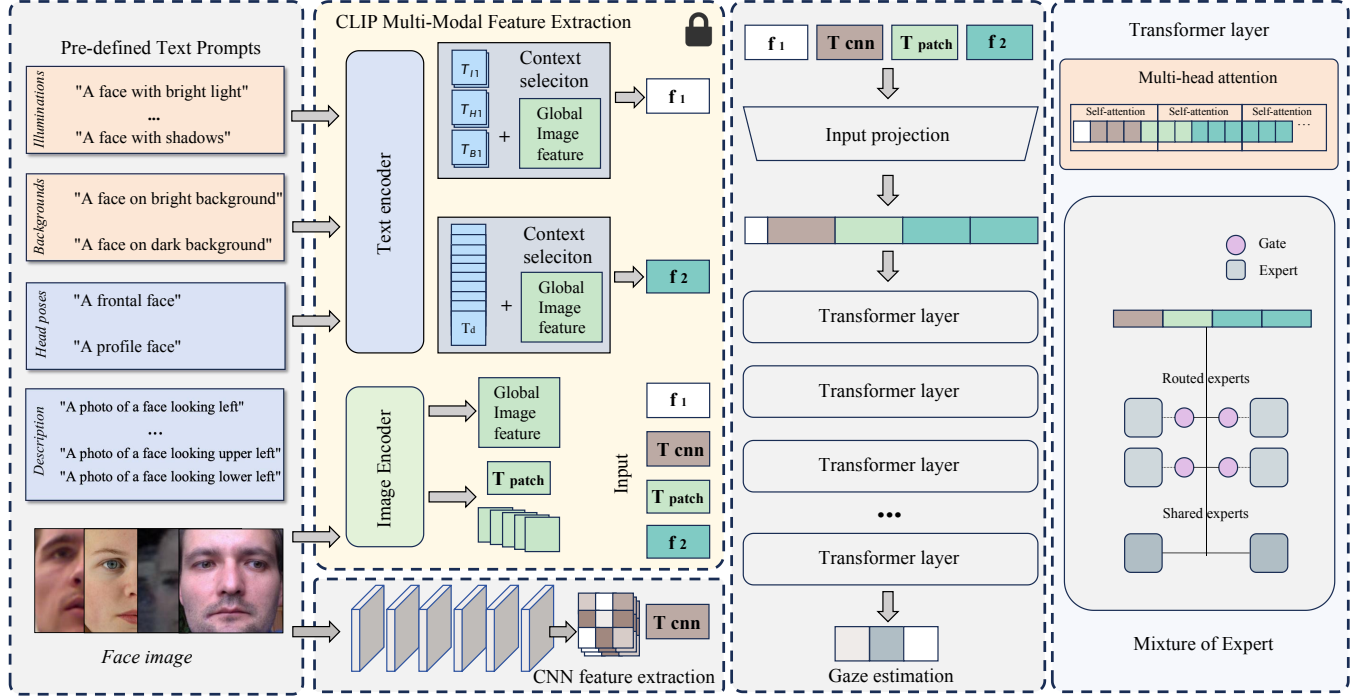


Fig. 1. (Left) CLIP Feature Extraction: A pre-trained CLIP text encoder processes four prompt categories (Illuminations, Backgrounds, Head Poses, Descriptions), which are fused with global image features via context selection to form semantic features f_1, f_2 . Meanwhile, a CNN extracts local visual maps. **(Right) Transformer Gaze Estimation:** Multi-modal features (f_1, f_2 , global patches T_{patch} , CNN features T_{cnn}) are projected, concatenated, and input into a Transformer encoder with MoE layers. The gating-based MoE enhances capacity and adaptability, yielding the final gaze prediction.

kens and high-resolution CNN features to estimate 3D gaze directions. The detailed process is summarized in Algorithm 1

2.1. Problem formulation

Given a face image $I \in \mathbb{R}^{H \times W \times 3}$ of height H and width W , the task is to predict a 3D unit gaze vector $\mathbf{g} \in \mathbb{R}^3$. We denote by \mathcal{E}_i a pre-trained CLIP vision encoder and by \mathcal{F}_{cnn} a trainable CNN backbone. From I , three types of features are extracted:

$$\begin{aligned} \mathbf{f}_{\text{global}} &= \mathcal{E}_i(I) \in \mathbb{R}^d, \\ \mathbf{T}_{\text{patch}} &= \{\mathbf{t}_1, \dots, \mathbf{t}_N\} \in \mathbb{R}^{N \times d}, \\ \mathbf{T}_{\text{cnn}} &= \text{Flatten}(\mathbf{F}_{\text{cnn}}) \in \mathbb{R}^{M \times C}, \end{aligned} \quad (1)$$

where $\mathbf{f}_{\text{global}}$ is the CLIP global embedding of dimension d , $\mathbf{T}_{\text{patch}}$ are N CLIP patch tokens, and \mathbf{T}_{cnn} are $M = H'W'$ tokens obtained by flattening the CNN feature map $\mathbf{F}_{\text{cnn}} \in \mathbb{R}^{H' \times W' \times C}$ with spatial size $H' \times W'$ and channel dimension C .

2.2. Context-aware semantic conditioning

We maintain learnable prototype banks \mathbf{P}_c for contexts $c \in \{\text{illum, head, bg, label}\}$. For each image, similarity scores s_c between the normalized global feature and prototypes are computed:

$$s_c = \text{softmax}(\tau \cdot (\hat{\mathbf{f}}_{\text{global}})(\hat{\mathbf{P}}_c)^\top), \quad (2)$$

where τ is a learnable temperature. We select the top prototype $p_c = \arg \max s_c$ and form two context-conditioned vectors:

$$\mathbf{f}_1 = \text{LayerNorm}\left(\mathbf{f}_{\text{global}} + \sum_{c \in \{\text{illum, head, bg}\}} \mathbf{P}_c[p_c]\right), \quad (3)$$

$$\mathbf{f}_2 = \text{LayerNorm}\left(\mathbf{f}_{\text{global}} + \mathbf{P}_{\text{label}}[p_{\text{label}}]\right).$$

This supplies sample-wise semantic priors without extra annotations.

2.3. Unified multi-scale token fusion

We concatenate the enriched global vectors with token sequences to form the Transformer input \mathcal{X} :

$$\mathcal{X} = [\mathbf{f}_1; \mathbf{f}_2; \mathbf{T}_{\text{patch}}; \mathbf{T}_{\text{cnn}}], \quad (4)$$

Algorithm 1 GazeFormer-MoE

Require: Image I , ground truth gaze \mathbf{g}
Ensure: Predicted gaze $\hat{\mathbf{g}}$

- 1: \triangleright 1. Extract multi-scale features from image I
- 2: $\mathbf{f}_{\text{global}}, \mathbf{T}_{\text{patch}} \leftarrow \mathcal{E}_i(I)$ \triangleright CLIP features
- 3: $\mathbf{T}_{\text{cnn}} \leftarrow \text{Flatten}(\mathcal{F}_{\text{cnn}}(I))$ \triangleright CNN features
- 4: \triangleright 2. Condition global feature with semantic prototypes
- 5: For each context c , select best prototype $\mathbf{P}_c[p_c]$ via similarity (Eq. 2)
- 6: Form two enriched vectors $\mathbf{f}_1, \mathbf{f}_2$ using the selected prototypes (Eq. 3)
- 7: \triangleright 3. Fuse tokens and process with MoE-Transformer
- 8: $\mathcal{X} \leftarrow \text{Concatenate}(\mathbf{f}_1, \mathbf{f}_2, \mathbf{T}_{\text{patch}}, \mathbf{T}_{\text{cnn}})$ \triangleright Create sequence (Eq. 4)
- 9: $\mathcal{Y} \leftarrow \text{MoE-Transformer}(\mathcal{X})$ \triangleright Apply MoE blocks (Eq. 5)
- 10: \triangleright 4. Predict gaze and compute loss
- 11: $\hat{\mathbf{g}} \leftarrow \text{PredictionHead}(\text{Pool}(\mathcal{Y}))$
- 12: $\mathcal{L}_{\text{total}} \leftarrow \mathcal{L}_{\text{ang}}(\hat{\mathbf{g}}, \mathbf{g}) + \text{regularizers}$ \triangleright Using angular loss (Eq. 6)
- 13: **return** $\hat{\mathbf{g}}$

2.4. Mixture of Experts Transformer

Our Transformer replaces feed-forward sublayers with gated MoE blocks. For token \mathcal{X} , routing produces sparse expert weights $r(\mathcal{X})$ and the MoE output is:

$$\text{MoE}(\mathcal{X}) = \sum_{i \in \text{TopK}(r(\mathcal{X}))} r_i(\mathcal{X}) \cdot \text{Expert}_i(\mathcal{X}). \quad (5)$$

We use a routed and shared design: a set of specialized experts (route dependent) plus shared experts for base capacity. Top-K, expert count E (refer to section 3.1), and the load-balancing loss follow standard practice.

2.5. Prediction head and training loss

The Transformer output is pooled and mapped to a 3D vector $\hat{\mathbf{g}}$. We train with an angular objective that is numerically stable:

$$\mathcal{L}_{\text{ang}}(\hat{\mathbf{g}}, \mathbf{g}) = 1 - \frac{\hat{\mathbf{g}}^\top \mathbf{g}}{\|\hat{\mathbf{g}}\| \|\mathbf{g}\|}, \quad (6)$$

which is monotone with the angular error and avoids explicit \arccos computation. We add standard regularizers (weight decay, MoE load balancing) and optimize with AdamW.

Table 1. Comparison of GE error (in degrees) on multiple datasets. Lower is better.

Methods	Pub. Year	M	E	G	Et
Gazenet [11]	TPAMI17	5.76°	6.79°	-	-
FullFace [6]	CVPR17	4.93°	6.53°	14.99°	7.38°
Dilated-Net [12]	ACCV19	4.42°	6.19°	13.73°	-
Gaze360 [13]	ICCV19	4.06°	5.36°	11.04°	11.04°
CA-Net [14]	AAAI 20	4.27°	5.27°	11.20°	-
AFF-Net [15]	ICPR 20	4.92°	6.41°	-	-
GazeTR-Hybrid [16]	ICPR 22	4.18°	5.44°	11.46°	-
GazeTr-Pure [17]	ICPR 22	4.24°	5.72°	13.58°	-
GazeCLIP [18]	arXiv 25	3.50°	4.70°	-	-
CLIP-DFENet [19]	arXiv 25	3.71°	4.97°	10.54°	-
MCA-PGI [20]	S. Reports	25.3	3.90°	4.58°	10.34°
GazeSymCAT [21]	JCDE 25	4.11°	5.13°	-	3.28°
IGTGGaze [22]	TIP 25	3.60°	4.56°	10.92°	-
PCNet [23]	TIP 25	3.99°	4.50°	-	4.00°
Ours	-	2.49°	3.22°	10.16°	1.44°

3. EXPERIMENT

3.1. Implementation Details

Experiments are conducted on NVIDIA RTX 4090 with PyTorch 2.4.1+cu124. The model combines CLIP ViT-B/32, ResNet-50, and a 12-layer MoE Transformer (8 heads, 512 dim, 2048 FFN), Top 4 experts. The MoE has 8 experts (4 active, 4 shared, 1024 FFN), with a unified feature dimension of 768. Training uses AdamW (LR $10^{-4} \rightarrow 10^{-6}$, cosine annealing), 100 epochs, batch size 128.

3.2. Datasets

We evaluate GazeFormer-MoE on four widely used GE benchmarks: EYEDIAP (**E**) [24], ETH-XGaze (**Et**) [25], Gaze360 (**G**) [13], and MPIIFaceGaze (**M**) [26]. These datasets jointly span controlled indoor setups, wide headpose and appearance variation, and in-the-wild conditions, enabling evaluation under diverse illumination, background, and pose regimes. Following the benchmark protocol of [5], we strictly divide the dataset into training validation and testing set with a ratio of 8 : 1 : 1.

3.3. Experimental results

Our method establishes new state of the art performance across all four benchmarks (Table 1). On **M** and **E** we reduce the best previously reported errors (3.5° / 4.50°) to 2.49° / 3.22°. **G** remains the most challenging; we still improve the strongest prior result (10.34°) to 10.16° while preserving robustness at large yaw. The largest absolute and relative gain appears on **E** (4.00° → 1.44°), consistent with our design goal of handling illumination and background diversity:

unified multi-scale token fusion plus routed and shared MoE markedly mitigates overfitting to studio-like lighting and captures fine periocular shading cues.

3.3.1. Ablation study

Table 2 shows that prototype-conditioned global vectors alone yield high errors, adding high-resolution CNN tokens produces the largest error collapse, and CLIP patch tokens provide the final consistent refinement. Table 3 isolates the effect of routed/shared MoE: removing MoE degrades performance across all benchmarks (most markedly on **E** and **M**), confirming that sparse conditional experts improve performance. Table 4 reports learning-rate sensitivity and identifies 10^{-4} as the best choice for stable convergence; both larger and smaller rates hurt accuracy.

Table 2. Experimental Results of Ablation Studies on Different Feature Combinations

Features combination	Datasets			
	M	E	G	Et
f_1	7.66°	10.25°	28.43°	10.75°
$f_1 + f_2$	7.72°	10.15°	27.70°	10.40°
$f_1 + f_2 + T_{cnn}$	3.20°	4.39°	10.92°	1.66°
$f_1 + f_2 + T_{cnn} + T_{patch}$	2.49°	3.22°	10.16°	1.44°

Table 3. Experimental Results of Ablation Studies on MoE Effect

MoE	Datasets			
	M	E	G	Et
+	2.49°	3.22°	10.16°	1.44°
w/o	4.20°	5.78°	10.72°	4.38°

Table 4. Experimental Results of Ablation Studies on Different Learning rate

Learning rate	Datasets			
	M	E	G	Et
10^{-3}	8.46°	11.30°	10.90°	4.66°
10^{-4}	2.49°	3.22°	10.16°	1.44°
10^{-5}	3.74°	7.70°	15.61°	1.84°
10^{-6}	5.39°	9.81°	15.89°	3.70°
10^{-7}	5.79°	10.37°	17.38°	4.23°

4. DISCUSSION

The evidence shows that coupling CLIP-aligned prototype conditioning with unified multi-scale token fusion and a routed/shared MoE materially reshapes the generalization profile of appearance-based gaze estimation under illumination, pose, and background shift. Achieving 2.49°, 3.22°, 10.16°, and 1.44° on datasets **M**, **E**, **G**, and **Et** respectively (up to 64% relative improvement over the strongest prior reports). Ablation studies clarify that the gains are not a simple depth or parameter scaling effect: prototype-conditioned

global tokens alone remain weakly constrained (errors above 7°, 10°, 28°, and 10° on the four datasets), indicating that coarse semantic priors without fine spatial structure under-express critical periocular micro-texture and shading cues; introducing high-resolution CNN tokens collapses much of this gap (e.g., **M** 7.66° to 3.20°), and the subsequent addition of CLIP patch tokens delivers a further consistent refinement (**M** 3.20° to 2.49°; **E** 4.39° to 3.22°), supporting the hypothesis that low-level texture, mid-level semantic structure, and prototype-guided context are complementary when co-attended within a single sequence space rather than fused late. Removing MoE produces uniform regressions (e.g., **Et** 1.44° to 4.38°), suggesting that a single dense feed-forward path simultaneously underfits rare, illumination-perturbed or high-yaw sub-distributions and overfits dominant frontal well-lit modes. The discrete prototype selection (argmax with learnable temperature) helps sharpen semantic routing and avoid noisy soft mixtures but imposes a finite granularity that may under-represent continuous illumination gradients or composite mixed-spectrum indoor–outdoor transitions; a static vocabulary also risks amplifying CLIP domain biases under sensor spectral shift (e.g., low-light color cast or infrared leakage). MoE introduces practical trade-offs: routing variance and potential tail latency under unbalanced expert loads, plus sensitivity to the load-balancing coefficient which, if mis-tuned, reduces capacity exactly where extreme yaw or deep shadow samples would benefit. Further, the present formulation is strictly single-frame and does not exploit temporal coherence (micro-saccades, blink dynamics, head micro-motion) that could regularize transient noise.

5. CONCLUSION

We presented GazeFormer-MoE, a semantics-modulated multi-scale Transformer that combines CLIP-driven prototype selection, unified fusion of prototype-enriched global vectors, CLIP patch tokens, and CNN tokens, and a routed and shared MoE to adapt capacity across different modalities. The model achieves state of the art errors of 2.49°, 3.22°, 10.16°, and 1.44° on datasets **M**, **E**, **G**, and **Et**, delivering up to 64% relative improvement. Ablations show (i) semantic prototypes alone are insufficient, (ii) cross-scale token unification supplies complementary texture and mid-level structure, and (iii) MoE routing is critical for handling long-tail (shadowed, extreme yaw) cases without overfitting dominant regimes. The approach remains limited by a static and discrete prototype vocabulary, single-frame processing, and routing overhead. Future directions include dynamic prototype evolution, temporally aware sparse experts, and latency-oriented expert distillation. Overall, results support semantic conditioning plus conditional capacity as a concise recipe for robust fine-grained geometric estimation.

6. COMPLIANCE WITH ETHICAL STANDARDS

This is a numerical simulation study for which no ethical approval was required.

7. REFERENCES

- [1] G. R. Chhipa, A. Kumar, S. Garhwal, F. Khan, Y.-K. Moon, *et al.*, “Revolutionizing gaze-based human-computer interaction using iris tracking: A webcam-based low-cost approach with calibration, regression and real-time re-calibration,” *IEEE Access*, 2024.
- [2] M. Jayalakshmi, T. P. Saradhi, S. M. R. Azam, S. Fazil, and S. D. S. Srinivas, “Multi-model human-computer interaction system with hand gesture and eye gesture control,” in *2024 5th International Conference on Innovative Trends in Information Technology (ICITHIT)*, pp. 1–6, IEEE, 2024.
- [3] N. Li, M. Chang, and A. Raychowdhury, “E-gaze: Gaze estimation with event camera,” *IEEE Transactions on Pattern Analysis and Machine Intelligence*, vol. 46, no. 7, pp. 4796–4811, 2024.
- [4] A. M. Mathew, A. A. Khan, T. Khalid, and R. Souissi, “Gescam: A dataset and method on gaze estimation for classroom attention measurement,” in *Proceedings of the IEEE/CVF Conference on Computer Vision and Pattern Recognition*, pp. 636–645, 2024.
- [5] Y. Cheng, H. Wang, Y. Bao, and F. Lu, “Appearance-based gaze estimation with deep learning: A review and benchmark,” *IEEE Transactions on Pattern Analysis and Machine Intelligence*, vol. 46, no. 12, pp. 7509–7528, 2024.
- [6] X. Zhang, Y. Sugano, M. Fritz, and A. Bulling, “It’s written all over your face: Full-face appearance-based gaze estimation,” in *Proceedings of the IEEE conference on computer vision and pattern recognition workshops*, pp. 51–60, 2017.
- [7] R. Liu, Y. Liu, H. Wang, and F. Lu, “Pnp-ga+: Plug-and-play domain adaptation for gaze estimation using model variants,” *IEEE Transactions on Pattern Analysis and Machine Intelligence*, vol. 46, no. 5, pp. 3707–3721, 2024.
- [8] A. Radford, J. W. Kim, C. Hallacy, A. Ramesh, G. Goh, S. Agarwal, G. Sastry, A. Askell, P. Mishkin, J. Clark, *et al.*, “Learning transferable visual models from natural language supervision,” in *International conference on machine learning*, pp. 8748–8763, PMLR, 2021.
- [9] W. Fedus, B. Zoph, and N. Shazeer, “Switch transformers: Scaling to trillion parameter models with simple and efficient sparsity,” *JMLR*, 2022.
- [10] C. Riquelme, J. Puigcerver, B. Mustafa, and *et al.*, “Scaling vision with sparse mixture of experts,” in *NeurIPS*, 2021.
- [11] R. Zemblys, D. C. Niehorster, and K. Holmqvist, “gazenet: End-to-end eye-movement event detection with deep neural networks,” *Behavior research methods*, vol. 51, no. 2, pp. 840–864, 2019.
- [12] Z. Chen and B. E. Shi, “Appearance-based gaze estimation using dilated-convolutions,” in *Asian Conference on Computer Vision*, pp. 309–324, Springer, 2018.
- [13] P. Kellnhofer, A. Recasens, S. Stent, W. Matusik, and A. Torralba, “Gaze360: Physically unconstrained gaze estimation in the wild,” in *Proceedings of the IEEE International Conference on Computer Vision (ICCV)*, pp. 2176–2184, IEEE, 2019.
- [14] R. Gu, G. Wang, T. Song, R. Huang, M. Aertsen, J. Deprest, S. Ourselin, T. Vercauteren, and S. Zhang, “Ca-net: Comprehensive attention convolutional neural networks for explainable medical image segmentation,” *IEEE transactions on medical imaging*, vol. 40, no. 2, pp. 699–711, 2020.
- [15] Y. Du, H. Chen, Y. Fu, J. Zhu, and H. Zeng, “Aff-net: A strip steel surface defect detection network via adaptive focusing features,” *IEEE Transactions on Instrumentation and Measurement*, vol. 73, pp. 1–14, 2024.
- [16] Y. Cheng and F. Lu, “Gaze estimation using transformer,” in *2022 26th International Conference on Pattern Recognition (ICPR)*, pp. 3341–3347, IEEE, 2022.
- [17] Y. Cheng and F. Lu, “Gaze estimation using transformer,” in *2022 26th International Conference on Pattern Recognition (ICPR)*, pp. 3341–3347, 2022.
- [18] J. Wang, H. Ruan, M. Wang, C. Zhang, H. Li, and J. Zhou, “Gazeclip: Towards enhancing gaze estimation via text guidance,” *arXiv preprint arXiv:2401.00260*, 2023.
- [19] L. Zhang, Y. Tian, W. Xu, Y. Jin, and Y. Huang, “Clip-driven dual feature enhancing network for gaze estimation,” *arXiv e-prints*, pp. arXiv–2502, 2025.
- [20] Y. Li, Y. Hong, Z. Wang, J. Chen, R. Liu, S. Ding, and B. Tan, “Non-linear multi-head cross-attention network and programmable gradient information for gaze estimation,” *Scientific Reports*, vol. 15, no. 1, p. 27135, 2025.
- [21] Y. Zhong and S. H. Lee, “Gazesymcat: A symmetric cross-attention transformer for robust gaze estimation under extreme head poses and gaze variations,” *Journal of Computational Design and Engineering*, vol. 12, no. 3, pp. 115–129, 2025.
- [22] W. Nie, Z. Wang, W. Ren, H. Zhang, and H. Liu, “Iris geometric transformation guided deep appearance-based gaze estimation,” *IEEE Transactions on Image Processing*, 2025.
- [23] Y. Tian, X. Wang, S. Zhang, W. Xu, Y. Jin, and Y. Huang, “‘disengage and integrate’: Personalized causal network for gaze estimation,” *IEEE Transactions on Image Processing*, 2025.
- [24] K. A. F. Mora, F. Monay, and J.-M. Odobez, “EYEDIAP: A database for the development and evaluation of gaze estimation algorithms from RGB and RGB-D cameras,” in *Proceedings of the ACM Symposium on Eye Tracking Research and Applications (ETRA)*, pp. 255–258, ACM, 2014.
- [25] X. Zhang, S. Park, T. Beeler, D. Bradley, S. Tang, and O. Hilliges, “ETH-XGaze: A large scale dataset for gaze estimation under extreme head pose and gaze variation,” in *Proceedings of the European Conference on Computer Vision (ECCV)*, pp. 365–381, Springer, 2020.
- [26] X. Zhang, Y. Sugano, M. Fritz, and A. Bulling, “It’s written all over your face: Full-face appearance-based gaze estimation,” in *Proceedings of the IEEE Conference on Computer Vision and Pattern Recognition Workshops (CVPRW)*, pp. 2299–2308, IEEE, 2017.